

Effects of 445-nm Laser on Vessels of Chick Chorioallantoic Membrane with Implications to Microlaryngeal Laser Surgery

Duy Duong Nguyen, MD, PhD ; Jing-Yin Pang, MBBS, MRCS, DOHNS, MMed;
Catherine Madill, PhD, CPSP ; Daniel Novakovic, FRACS, MBBS, MPH 

Objective: Previous research has shown that effective application of angiolytic lasers in microlaryngeal surgery is determined by wavelength, pulse width (PW), and fluence. Recently, a 445-nm (blue) laser (BL) has been developed with a potentially greater hemoglobin absorption than previous lasers. The chick chorioallantoic membrane (CAM) represents a suitable model for testing various settings to find out the most optimal settings of this laser. This study used the CAM model to examine whether successful photoangiolytic effects could be obtained using BL.

Methods: Seven hundred and ninety three third-order vascular segments of viable CAM were irradiated using BL via 400- μ m diameter fiber, 1 pulse/second, with PW and power varied systematically at standardized fiber-to-vessel distances of 1 and 3 mm. Outcome measures including vessel ablation rate (AR), rupture rate (RR), and visible tissue effects were analyzed using Chi-square test.

Results: Energy levels of 400, 540, and 600 mJ (per pulse) were most effective for vessel ablation. A working distance of 3 mm resulted in higher ablation and less vessel rupture compared with 1 mm at these optimal energy levels. At 3 mm, a longer PW resulted in higher AR. At 1 mm, AR increased with shorter PW and higher power. The 1-mm working distance resulted in lower tissue effects than 3 mm.

Conclusion: Findings in this study showed that BL was effective in vessel ablation using relevant combination of working distance, PW, and energy levels. To obtain high AR, longer working distance plus longer PW was required and if working distance was reduced, shorter PW should be set.

Key Words: Blue laser, 445-nm laser, photoangiolysis, microlaryngeal surgery, chick chorioallantoic membrane.

Level of Evidence: NA

Laryngoscope, 131:E1950–E1956, 2021

INTRODUCTION

Laser application in surgery has been based on selective (photoangiolytic) or non-selective (cutting) light wavelength absorption by the target tissue.^{1,2} Angiolytic lasers use hemoglobin as the chromophore¹ the absorption coefficient curve of which has peaks at 418 nanometers (nm), 524, 577, and 1,064 nm^{3,4} (Fig. 1). Vascular effects occur as energy at a given wavelength, which is preferentially absorbed by hemoglobin over adjacent tissues.⁵

This is an open access article under the terms of the Creative Commons Attribution-NonCommercial-NoDerivs License, which permits use and distribution in any medium, provided the original work is properly cited, the use is non-commercial and no modifications or adaptations are made.

From the Voice Research Laboratory, Susan Wakil Health Building, Faculty of Medicine and Health (D.D.N., C.M., D.N.), The University of Sydney, Camperdown, New South Wales, Australia; Department of ENT (J.-Y.P.), Khoo Teck Puat Hospital, Singapore; and the Department of Otolaryngology—Head and Neck Surgery (D.N.), The Canterbury Hospital, Campsie, New South Wales, Australia.

Additional supporting information may be found in the online version of this article.

Editor's Note: This Manuscript was accepted for publication on December 17, 2020.

This study was supported by the Dr Liang Voice Program, The University of Sydney. The authors have no other funding, financial relationships, or conflicts of interest to disclose.

Send correspondence to Daniel Novakovic, FRACS, MBBS, MPH, Suite 1, Level 1, 66 Pacific Highway, St Leonards, NSW 2065, Australia. E-mail: daniel.novakovic@sydney.edu.au

DOI: 10.1002/lary.29354

Photoangiolysis allows treatment of vascular lesions that affect vibratory characteristics of the delicate vocal fold mucosa while preserving its ultrastructure and pliability which is important especially in professional voice users.⁶ Animal⁷ and clinical studies⁸⁻¹⁰ have demonstrated the effectiveness of angiolytic lasers in treatment of vocal fold varices,⁶ polyps,^{10,11} papillomatosis,^{8,12} and dysplasia.¹³

In microsurgery using angiolytic laser, there is a range of effects upon blood vessels¹⁴ where the two most clinically significant endpoints are vessel ablation (vascular occlusion) and rupture² where vessel contents extravasate into surrounding tissues. Vessel ablation is desirable in phonosurgery as hemorrhage from a ruptured vessel can have negative impact upon the laser procedure and potentially surgical outcome.¹⁵ If hemorrhage occurs, the laser energy is absorbed by more superficial blood rather than the sub-lesion or intra-lesion microcirculation.¹⁶ In addition, blood extravasation into the superficial lamina propria can result in indiscriminate absorption of laser energy causing photothermal trauma to this structure.¹⁵ Factors that affect these outcomes include laser wavelength,¹⁷ vessel diameter,¹⁸ pulse width (PW),¹⁴ and fluence.^{14,19} While wavelength for a given laser is fixed, its PW, power, and working distance can be manipulated by the surgeon to affect the energy delivered per unit area (pulse fluence). Therefore, it is important to determine the most optimal combination of settings.

Several angiolytic lasers have been used in microlaryngeal surgery. The 585-nm pulsed dye laser (PDL)^{20,21} has very short PW resulting in variable coagulation² and high incidence of vessel rupture,¹⁶ thus decreasing vascular selectivity.¹⁵ The 532-nm pulsed potassium-titanyl-phosphate (KTP) laser (Aura XP™—Boston Scientific, MA, USA) has more selective absorption of hemoglobin at this wavelength⁸ and longer PW than the PDL¹⁶ making it more effective in selective photoangiolytic.¹⁵ However, this laser is sensitive to mechanical impact, is expensive to maintain, has limited pulse duration options, and future availability and support may be limited.

Recently, a novel 445-nm laser has been developed for clinical use (WOLF TruBlue laser, A.R.C. Laser GmbH, Nuremberg, Germany).^{22,23} This laser was claimed to have a number of advantages over KTP laser: 1) A stronger tissue effect with the same pulse and energy settings (due to a higher hemoglobin absorption peak)⁴ (Fig. 1), 2) Wide range of pulse rates from continuous wave to less than a millisecond (ms), 3) Better cutting ability, and 4) Wider application in microlaryngeal surgery.²² To date, no study has experimentally evaluated the effects of the 445-nm laser on microvasculature and whether it offers comparable vascular ablation capability.

Laboratory-controlled experimental conditions allow investigation of laser settings applicable to microlaryngeal surgery while minimizing confounding factors. The chick chorioallantoic membrane (CAM) is an insensate membrane in the chick embryo. From day 15 of the embryonic period, the CAM has branching blood vessels of various diameters. The CAM can be exposed by removing the top of the eggshell allowing easy identification of and access to blood vessels through the thin membrane. The diameter and structure of blood vessels in the CAM are also highly similar to those of the human vocal folds, making the CAM an excellent experimental model to examine the effects of angiolytic lasers.² Previous studies have used the CAM model to test the 585-nm PDL² and 532-nm pulsed KTP.^{2,15} To date, no studies have examined the effects of blue laser (BL) on CAM to suggest optimal settings to achieve high vessel ablation rate (AR) and low rupture rate (RR), or examined the effects of changes in working distance, PW, and power upon the vascular endpoints. This study of BL on CAM vessels aimed to 1) Identify settings with high AR; and 2) Examine effects of varying working distance and PW.

MATERIALS AND METHODS

Ethical Approval

This study was approved by the Sydney Local Health District Animal Welfare Committee (protocol number: 2019/006A). All guidelines and regulations governing research in animals were followed.

Protocols

Fertilized chicken eggs were incubated at 37.4°C and 65% relative humidity using an egg incubator (Type Janoel JN8-48). On day 12–14 of the incubation period, eggs were removed from the incubator and placed on a laboratory cup in vertical position

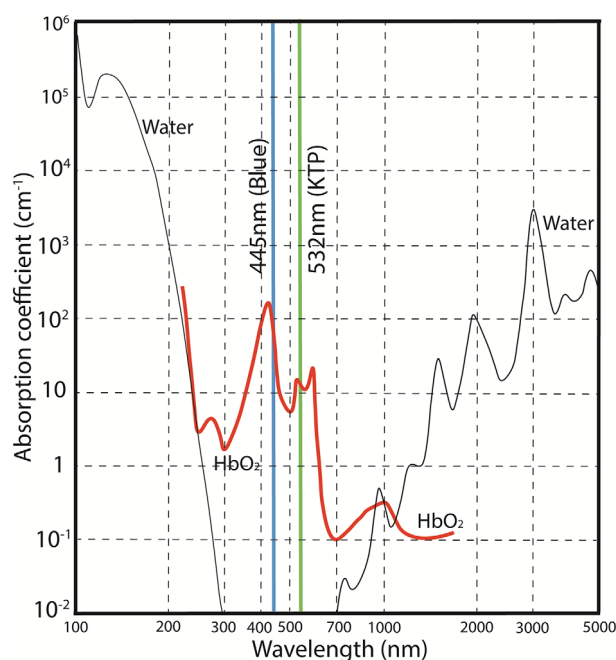


Fig. 1. Absorption coefficient spectrum of oxyhemoglobin (HbO₂) and water. Adapted from ref. [4] nm = nanometer.

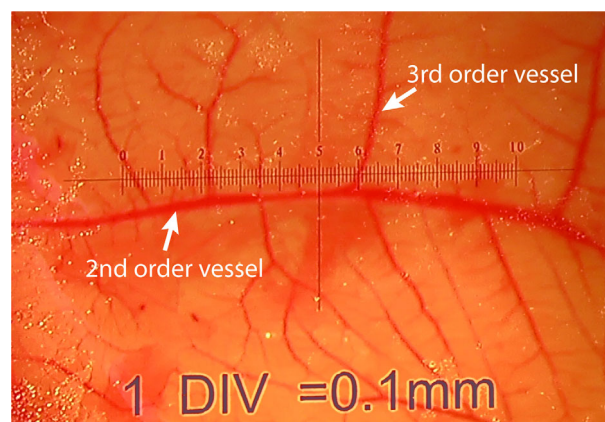


Fig. 2. Measurement of vessel diameter using a calibrated micrometer.

for 20 minutes to acclimatize eggs with the room environment. The top of the eggshell was carefully removed to expose the CAM. Dissection was performed under surgical microscope to expose the vascularized layer. Anesthesia was given topically to the CAM using medetomidine solution 1 mg/mL diluted to 1:100 in saline (0.9% NaCl) at a dosage of 0.3 mg/kg, as described by Waschkie et al.²⁴

Three types of the blood vessels differing in diameter were identified: a primary vessel (i.e. the largest vessel), second-order vessels branching from the primary vessel, and third-order vessels branching from second-order vessels.¹⁵ A precise micrometer was used to measure vessel diameter with the assistance of video-editing software (Fig. 2).

Laser experiments were performed using a WOLF TruBlue™ 445-nm surgical laser system.²³ Laser was deployed via a 400-μm

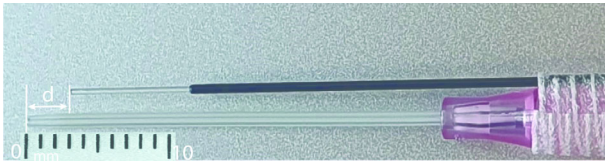


Fig. 3. Set-up with the laser fiber taped to a plastic cannula to maintain the minimum working distance; d = distance between the tips of the fiber and the cannula.

fiber at a rate of one pulse/second (s). This fiber size was chosen as it was the first clinically available and most commonly produced fiber for the blue laser and also allowed comparison with previous blue and KTP laser experiments using this size.^{2,22} A Carl Zeiss OPMI pico surgical microscope²⁵ with laser filter for eye protection coupled with a camera head (Panasonic GP-US932)²⁶ connected to a video capture device (Smith & Nephew 660HD)²⁷ was used for the experiment. All staff used protective goggles and followed laser safety regulations. Third-order vessels in the CAM were irradiated with 445-nm light at fiber-to-tissue distances of 1 or 3 mm. The laser fiber was taped to the hub of a plastic cannula, the tip of which extended 1 or 3 mm beyond the tip of the laser fiber (Fig. 3). The fiber and the cannula were parallel so that when the cannula tip was in contact with the CAM in a perpendicular angle, the desired tip-to-target distance was achieved.

At each working distance, a combination of PW and power was tested using a number of vascular segments (Tables S1 and S2). Energy was delivered until the vessel was ablated or ruptured. Ablation was defined as a complete seal of the vessel wall with coagulation of intraluminal blood, creating a bloodless vascular segment.¹⁵ Rupture was defined as an extravasation of blood into the surrounding area.¹⁵ The outcome 'no effects' was recorded after 10 pulses without any identifiable ablation or rupture.² Thermal effects on surrounding tissue were also recorded and were defined as tissue carbonization that occurred in the CAM membrane area adjacent to the spot under target. If there was a combination of both rupture and ablation, the outcome was categorized as rupture. All outcome measures (ablation, rupture, and tissue effects) were ascertained using microscopic visualization. Histopathology confirmation of outcome measures was deemed impossible because a large number of vascular segments were used, and biopsy could cause bleeding of adjacent CAM vessel that could interfere with the experiment. The percentage (%) of each outcome (AR, RR, and tissue effects) was calculated by dividing the number of vascular segments with the observed outcome by the total number of vascular segments used for each setting and multiplied by 100.

Dependent variables included: 1) AR (%); 2) RR (%); and 3) Tissue effect (%). Independent variables included: 1) PW (millisecond, ms); 2) Fiber-to-target working distance (millimeter, mm); 3) Power (Watts, W); 4) Energy level per pulse (millijoules, mJ) calculated as pulse width x power; 5) Vessel diameter (mm); and 6) Fluence (joules per square centimeter, J/cm^2).

Carbon debris and incorrect cleaving of the laser fiber can affect the irradiated energy resulting in unpredictable angiolytic effects.²⁸ Therefore, caution was taken during the experiment to ensure the fiber was regularly cleaved as per manufacturer instructions.

Statistical Analyses

Data were managed in Microsoft Excel and analyzed using SPSS 25.0.²⁹ Chi-square test was used to compare the rate of vessel rupture, vessel ablation, and thermal tissue effects

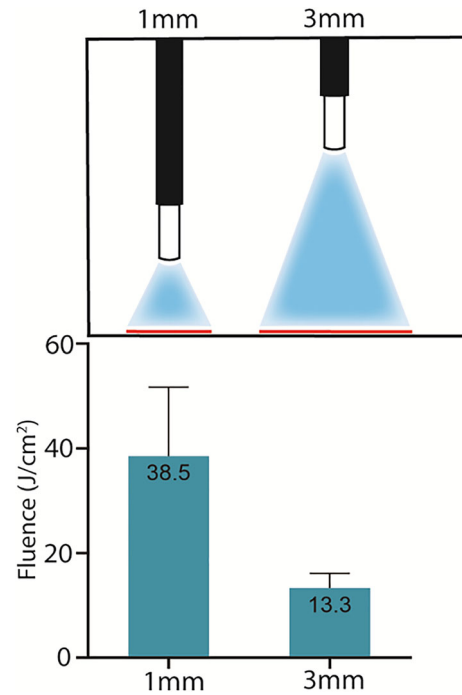


Fig. 4. Exposure spot (upper panel) and pulse fluence (lower panel) at the two working distances for 400- μ m fiber. Error bars indicate standard deviation.

between different laser settings and working distances. A significance level of 0.05 was used.

RESULTS

Seven hundred and ninety three third-order vascular segments of viable CAM from 63 chick embryos (average weight = 54.3 g) were tested. Mean diameter of vessels was 0.11 mm (SD = 0.03; 95% CI = 0.1–0.12; range = 0.06–0.18 mm). Vessels with diameters from 0.1 to 0.2 mm are reported to have a thermal relaxation time of approximately 4.8–19.0 ms.¹⁹ Figure 4 shows mean fluence for the two working distances. Mean (SD) of exposure spot (mm) at 1 and 3 mm was 1.3 (0.21) and 2.17 (0.26), respectively.

Settings with High AR

Figure 5 shows AR and RR for all tested energy levels at two working distances. The number of vascular segments used for these settings is shown in Tables S1 and S2. Overall, this laser was effective in ablating vessels of the CAM with longer working distance (3 mm) apparently resulting higher AR and low RR than short working distance (1 mm). The angiolytic effects also appeared to be different across energy level. At very low energy (320 mJ/4 w/80 ms and 360 mJ/4 w/90 ms) AR was low at both 1 and 3 mm. From 400 mJ, high AR was observed at both working distances, especially at high energy (540 and 600 mJ). Figure 5 also shows that the settings of energy per pulse for the most effective vascular ablation are 400 mJ (10 w \times 40 ms at 1 mm and 4 w \times 100 ms at 3 mm), 540 mJ (9 w \times 60 ms at

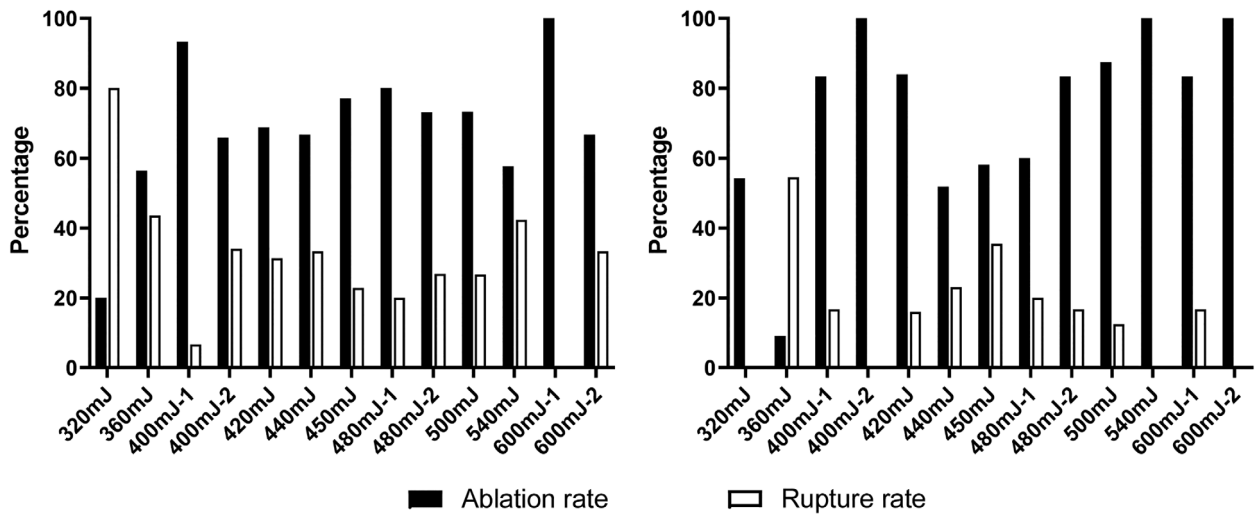


Fig. 5. Percentage of ablation rate and rupture rate for tested energy levels at two working distances. $400\text{ mJ}^{-1} = 10\text{ w} \times 40\text{ ms}$; $400\text{ mJ}^{-2} = 4\text{ w} \times 100\text{ ms}$; $480\text{ mJ}^{-1} = 4\text{ w} \times 120\text{ ms}$; $480\text{ mJ}^{-2} = 8\text{ w} \times 60\text{ ms}$; $600\text{ mJ}^{-1} = 10\text{ w} \times 60\text{ ms}$; $600\text{ mJ}^{-2} = 4\text{ w} \times 150\text{ ms}$.

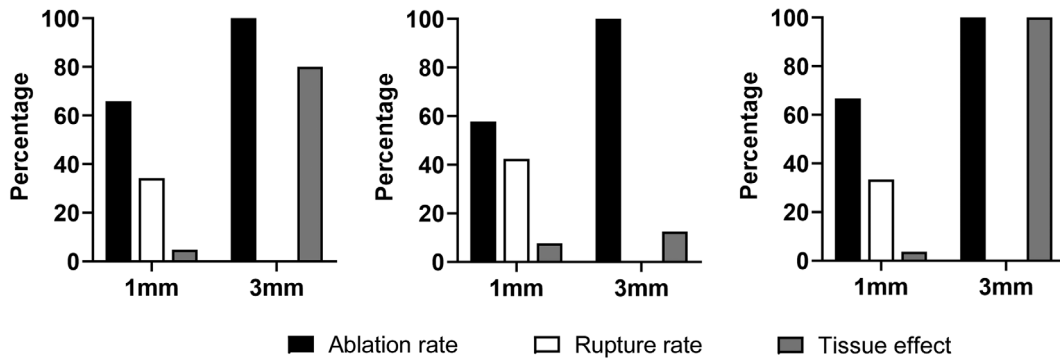


Fig. 6. Effects of working distance. Rupture rate was 0% at 3 mm for all three energy levels.

3 mm), and 600 mJ (10 w × 60 ms at 1 mm and 4 w × 150 ms at 3 mm).

Effects of Working Distance

Given the different trends in angiolytic effects observed between the two working distances as shown in Figure 5, AR and RR were compared between 3 and 1 mm while keeping PW and power constant. The effects of working distances are shown in Figure 6. Longer working distance (3 mm vs 1 mm) resulted in higher ablation and less vessel ruptures at 400 mJ (4 w, 100 ms, $\chi^2 = 6.829$, $P = .009$), 540 mJ (9 w, 60 ms, $\chi^2 = 13.018$, $P = .000$), and 600 mJ (4 w, 150 ms, $\chi^2 = 9.714$, $P = .002$).

Longer working distance also resulted in a higher rate of visible tissue effects at 400 mJ (4 w, 100 ms, $\chi^2 = 33.054$, $P = .000$) and 600 mJ (4 w, 150 ms, $\chi^2 = 47.147$, $P = .000$) but not at 540 mJ (9 w, 60 ms, $P = .6$).

Effects of PW

PW was switched between short and long for the two energy levels with highest AR (400 and 600 mJ) at both

1 and 3 mm. The effects of PW on ablation, rupture, and tissue are shown in Figure 7 and are described as follows:

At long working distance (3 mm). Longer PW resulted in higher AR and lower RR at both 400 and 600 mJ. At 400 mJ when PW increased from 40 ms (n = 24) to 100 ms (n = 15) AR increased from 83.3% to 100% and RR decreased from 16.7% to 0%, however this was not statistically significant ($P = .095$). At 600 mJ when PW increased from 60 ms (n = 24) to 150 ms (n = 24) AR increased from 83.3% to 100% and RR decreased from 16.7% to 0% ($\chi^2 = 4.364$, $P = .037$).

Longer PW also resulted in greater visual tissue effects. At 400 mJ, rate of tissue effects was 33.3% at 40 ms but increased to 80% at 100 ms ($\chi^2 = 8.046$, $P = .005$). At 600 mJ, rate of tissue effects increased from 41.7% at 60 ms to 100% at 150 ms ($\chi^2 = 19.765$, $P = .000$).

At short working distance (1 mm). At the short working distance, the effect of varying PW was contrary to that in the long working distance. In particular, at 1 mm increasing PW significantly decreased AR and increased RR at both 400 and 600 mJ. At 400 mJ, when PW increased from 40 ms (n = 30) to 100 ms (n = 41) AR decreased from 93.3% to 65.9% and RR increased from 6.7% to 34.1% ($\chi^2 = 7.494$, $P = .006$). At 600 mJ, when PW

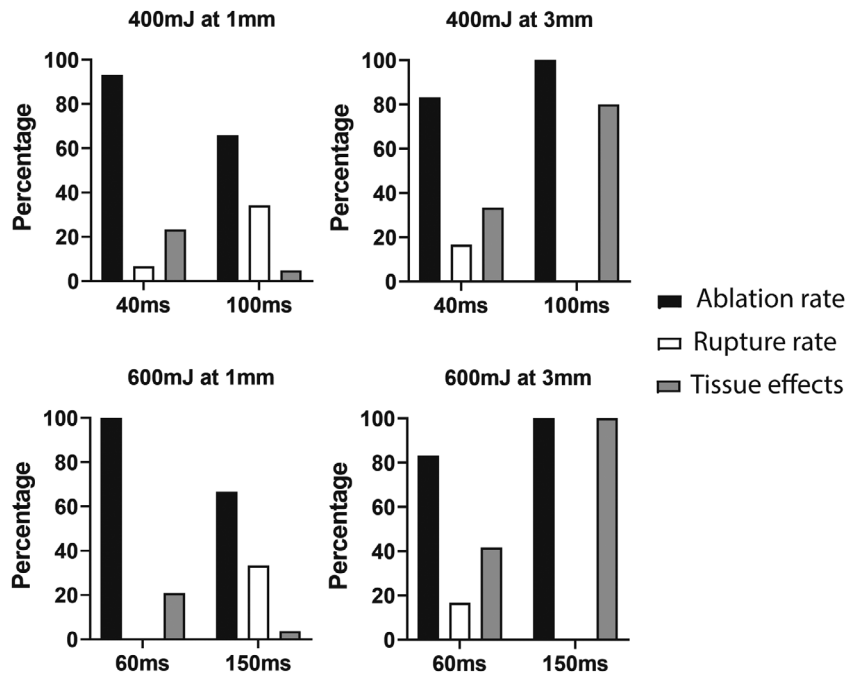


Fig. 7. Effects of varying pulse width.

increased from 60 ms (n = 24) to 150 ms (n = 27) AR decreased from 100% to 66.7% while RR increased from 0% to 33.3% ($\chi^2 = 9.714$, $P = .002$).

At 1 mm increasing PW also resulted in lower rate of tissue effects. At 400 mJ, tissue effects was 23.3% at 40 ms but dropped to 4.9% at 100 ms ($\chi^2 = 5.331$, $P = .021$). At 600 mJ, tissue effects were observed in 20.8% at 60 ms but showed a trend of lower rate (3.7%) at 150 ms ($\chi^2 = 3.592$, $P = .058$).

DISCUSSION

This study simulated microlaryngeal conditions using different combinations of PW, fiber-to-target working distance, and power of BL on the vascularity of the CAM model. Third-order vessels (allowing comparison with previous CAM model laser studies)¹⁵ had an average diameter of 0.11 mm which is similar to the size of superficial blood vessels of the human vocal fold (range = 0.015–0.1 mm).³⁰ While larger CAM vessels (first order and second order) may better represent vascular lesions e.g. varices, they were not investigated in this study. Findings showed that this laser obtained high AR across a wide range of energy levels at both 1 mm and 3 mm.

PW is an important parameter of angiolytic lasers and research has shown that long PW is advantageous³¹ as extremely short PWs are associated with higher rates of vessel rupture (PDL³²) than long PW (KTP laser¹⁶). Compared with PDL and pulsed KTP lasers, the BL used in this study offers a wider range of operating pulse widths from 1 ms to 45 s/continuous wave.²³ In the platform tested at the higher power settings (4.5–10 w) only short pulses (max 60 ms) can be used which is why our maximum energy delivery was limited to 600 mJ per pulse. At

the lower power settings (4 w and below) a longer PW (up to 150 ms) can be set. Data from two energy levels with highest AR (400 and 600 mJ, Fig. 7) showed that the effects of PW variation were different between 3 and 1 mm working distances. We observed high ablation and low rupture using long PW at 3 mm. However, at 1 mm increasing PW significantly decreased AR and increased RR, probably due to higher pulse fluence. The fact that angiolytic effects depend upon pulse fluence has been documented in studies with KTP laser^{2,15} and BL.²² A combination of laser energy and fiber-to-tissue working distance determines its fluence.¹⁵ Our experimental data showed slightly higher mean fluence than previously reported for both working distances²² (Fig. 4). The higher AR at 3 mm implied that lower pulse fluence appeared to be more optimal for BL. The two working distances used in this study were 1 and 3 mm to allow comparison with previous reports on KTP laser¹⁵ and these are also used frequently in microlaryngeal surgery. Our findings showed that angiolytic effects of BL were determined by both PW and working distance. For complete vessel ablation, long pulse widths at long (3 mm) distance were required and if working distance was reduced, shorter pulse widths would be required.

Using 532-nm pulsed-KTP laser on CAM vessels,¹⁵ Broadhurst et al showed that longer PW resulted in less vessel ruptures at 1 mm and 550 mJ. At the same energy level at 3 mm, they found that increasing PW did not result in vessel rupture. Only our results at 3 mm agreed with these findings while the data at 1 mm showed a contrary trend. PW essentially stipulates the time the vessel is exposed to the laser energy and should be compatible with the vessel diameter and approximately equal to the thermal relaxation time of

that diameter.³³ Using 532 and 1,064 nm laser energy, Suthamjariya et al.¹⁴ have shown that by increasing pulse width, the threshold fluence for angiolytic effects increased, leading to less vessel rupture. They recommended that pulses between 10 and 30 ms are most suitable for effective photoangiolytic of 0.12-mm to 0.15-mm vessel size. This is also the typical pulse width range of KTP laser in microlaryngeal surgery. Experiments on KTP laser mostly found great ablation/low rupture rate when increasing pulse width within this range.^{2,15} In the present study, the effective PW settings of BL were much higher than the optimal pulse width range of KTP laser as mentioned above. If PW is longer than thermal relaxation time of the vessels, the effects would be non-specific thermal damage instead of effective coagulation.³⁴ This may be a reason for different patterns of vessel-laser interaction of BL compared with KTP. Additionally, previous research has shown correlation of vessel damage with laser wavelength.¹⁷ Although BL and KTP lasers may be functionally similar in terms of angiolytic effects, there are differences in oxyhemoglobin optical absorption between the 445 nm of BL and 532 nm of KTP⁴ with 445 nm light having a higher affinity compared with 532 nm light (Fig. 1).

In this study, we also found that visible surface tissue effects were significantly greater at 3 mm than at 1 mm. This may be related to the longer PW and hence a longer exposure time.³⁴ Additionally, the larger exposure spot diameter at 3 mm provides a larger surface area for laser-tissue interaction, possibly making laser-tissue interactions more visible. The greater tissue effect at 3 mm was observed at the surface of the CAM. It is unclear whether this is relevant when translated to a clinical setting. A possible implication is that longer working distances might be more relevant for superficial epithelial lesions e.g. laryngeal papillomatosis.

In summary, given that BL was effective in ablating blood vessels in the CAM model, it is expected that this laser is also successful in treatment of the types of vocal fold lesions that have been treated using previous angiolytic lasers e.g. varices,⁶ polyps,¹⁰ papillomatosis.^{8,12} Clinical studies are needed to examine the effects of the blue laser on these lesions.

CONCLUSION

The following points can be withdrawn from this study:

1. BL was highly effective in ablating vessels of the CAM model. Higher ablation rates and lower vessel rupture rates were observed at the 3 mm working distance compared with the 1 mm working distance.
2. At 3 mm working distance, longer PW resulted in higher AR lower RR. Effective PW settings of BL for angiolytic were higher than reported PW ranges of other angiolytic lasers, suggesting differences in vessel-laser interaction across lasers.
3. Lower energy levels less than 400 mJ per pulse are ineffective for vascular ablation and may lead to increased risk of vessel rupture. The most effective

energy levels for vascular ablation are 400, 540, and 600 mJ.

4. At a working distance of 1 mm, a shorter PW and higher power is required to achieve high AR at equivalent energy levels.
5. Visible tissue effects are lower at 1 mm compared with 3 mm working distances.

These findings imply that the 445 nm Blue laser is likely to be effective in treatment of types of vocal fold lesions that have been successfully treated using other angiolytic lasers.

ACKNOWLEDGMENTS

We would like to thank Suzanne Pears (Director of Animal Care, Sydney Local Health District), Innes Wise (Laboratory Animal Services, Charles Perkins Centre, The University of Sydney), and Mikala Welsh (The Animal House, Royal Prince Alfred Hospital, Sydney) for their support during our laser experiments.

BIBLIOGRAPHY

1. Azadgoli B, Baker RY. Laser applications in surgery. *Ann Transl Med* 2016; 4:452.
2. Burns JA, Kobler JB, Heaton JT, Anderson RR, Zeitels SM. Predicting clinical efficacy of photoangiolytic and cutting/ablating lasers using the chick chorioallantoic membrane model: implications for endoscopic voice surgery. *Laryngoscope* 2008;118:1109–1124.
3. Patil UA, Dharmi LD. Overview of lasers. *Indian J Plastic Surg* 2008;41: S101–S113.
4. Boulnois J-L. Photophysical processes in recent medical laser developments: a review. *Lasers Med Sci* 1986;1:47–66.
5. Anderson RR, Jaenicke KF, Parrish JA. Mechanisms of selective vascular changes caused by dye lasers. *Lasers Surg Med* 1983;3:211–215.
6. Zeitels SM, Akst LM, Burns JA, et al. Pulsed angiolytic laser treatment of ectasias and varices in singers. *Ann Otol Rhinol Laryngol* 2006;115: 571–580.
7. Novakovic D, D'Elia J, Branski RC, et al. The effect of different angiolytic lasers on resolution of subepithelial mucosal hematoma in an animal model. *Ann Otol Rhinol Laryngol* 2014;123:387–394.
8. Zeitels SM, Burns JA. Office-based laryngeal laser surgery with the 532-nm pulsed-potassium-titanyl-phosphate laser. *Curr Opin Otolaryngol Head Neck Surg* 2007;15:394–400.
9. Kishimoto Y, Hirano S, Kato N, Suehiro A, Kanemaru SI, Ito J. Endoscopic KTP laser photocoagulation therapy for pharyngolaryngeal venous malformations in adults. *Ann Otol Rhinol Laryngol* 2008;117:881–885.
10. Ivey CM, Woo P, Altman KW, Shapshay SM. Office pulsed dye laser treatment for benign laryngeal vascular polyps: a preliminary study. *Ann Otol Rhinol Laryngol* 2008;117:353–358.
11. Mizuta M, Hiwatashi N, Kobayashi T, Kaneko M, Tateya I, Hirano S. Comparison of vocal outcomes after angiolytic laser surgery and microflap surgery for vocal polyps. *Auris Nasus Larynx* 2015;42:453–457.
12. Maturo S, Hartnick CJ. Use of 532-nm pulsed potassium titanil phosphate laser and adjuvant intralesional bevacizumab for aggressive respiratory papillomatosis in children: initial experience. *Arch Otolaryngol Head Neck Surg* 2010;136:561–565.
13. Burns JA, Friedman AD, Lutch MJ, Hillman RE, Zeitels SM. Value and utility of 532 nanometre pulsed potassium-titanil-phosphate laser in endoscopic laryngeal surgery. *J Laryngol Otol* 2010;124:407–411.
14. Suthamjariya K, Farinelli WA, Koh W, Rox Anderson R. Mechanisms of microvascular response to laser pulses. *J Invest Dermatol* 2004;122:518–525.
15. Broadhurst MS, Akst LM, Burns JA, et al. Effects of 532 nm pulsed-KTP laser parameters on vessel ablation in the avian chorioallantoic membrane: implications for vocal fold mucosa. *Laryngoscope* 2007;117: 220–225.
16. Zeitels SM, Akst LM, Burns JA, Hillman RE, Broadhurst MS, Anderson RR. Office-based 532-nm pulsed KTP laser treatment of glottal papillomatosis and dysplasia. *Ann Otol Rhinol Laryngol* 2006;115: 679–685.
17. Kimel S, Svaasand LO, Hammer-Wilson MJ, Nelson JS. Influence of wavelength on response to laser photothermolysis of blood vessels: implications for port wine stain laser therapy. *Lasers Surg Med* 2003;33:288–295.
18. Kimel S, Svaasand LO, Hammer-Wilson M, et al. Differential vascular response to laser photothermolysis. *J Invest Dermatol* 1994;103:693–700.

19. Anderson RR, Parrish JA. Microvasculature can be selectively damaged using dye lasers: a basic theory and experimental evidence in human skin. *Lasers Surg Med* 1981;1:263–276.
20. Franco RA Jr, Zeitels SM, Farinelli WA, Faquin W, Anderson RR. 585-nm pulsed dye laser treatment of glottal dysplasia. *Ann Otol Rhinol Laryngol* 2003;112:751–758.
21. Franco RA Jr, Zeitels SM, Farinelli WA, et al. 585-nm pulsed dye laser treatment of glottal papillomatosis. *Ann Otol Rhinol Laryngol* 2002;111:486–492.
22. Hess MM, Fleischer S, Ernstberger M. New 445 nm blue laser for laryngeal surgery combines photoangiolytic and cutting properties. *Eur Arch Otorhinolaryngol* 2018;275:1557–1567.
23. A.R.C. Laser GmbH. Wolf trublue 2020. Available at: <https://www.arclaser.de/en/products/trublue/wolf-trublue/>. Accessed November 1, 2020.
24. Waschkes C, Nicholls F, Buschmann J. Comparison of medetomidine, thiopental and ketamine/midazolam anesthesia in chick embryos for in ovo magnetic resonance imaging free of motion artifacts. *Sci Rep* 2015;5:15536.
25. ZEISS. ZEISS OPMI Pico. Available at: <https://www.zeiss.com/meditec/int/product-portfolio/surgical-microscopes/opmi-pico.html>. Accessed November 1, 2020.
26. Panasonic Asia Pacific. Panasonic 3MOS OEM Micro Camera Solution GP-US932. Available at: <https://business.panasonic.com.au/professional-camera/micro-cameras/panasonic-3mos-oem-micro-camera-solution-gp-us932#>. Accessed November 1, 2020.
27. Smith & Nephew, Inc. 660HD Image Management System. Available at: <https://www.smith-nephew.com/professional/products/all-products/660-hd/>. Accessed November 1, 2020.
28. Tracy LF, Kobler JB, Van Stan JH, et al. Carbon debris and fiber cleaving: effects on potassium-titanyl-phosphate laser energy and chorioallantoic membrane model vessel coagulation. *Laryngoscope* 2019;129:2244–2248.
29. IBM Corp. IBM SPSS Software 2018. Available at: <https://www.ibm.com/analytics/data-science/predictive-analytics/spss-statistical-software>. Accessed November 1, 2020.
30. Broadhurst MS, Kobler JB, Burns JA, Anderson RR, Zeitels SM. Chick chorioallantoic membrane as a model for simulating human true vocal folds. *Ann Otol Rhinol Laryngol* 2007;116:917–921.
31. Koufman J, Zeitels S, Anderson R, et al. Letters to the editor. *Ann Otol Rhinol Laryngol* 2007;116:317–318.
32. Zeitels SM, Franco RA Jr, Dailey SH, et al. Office-based treatment of glottal dysplasia and papillomatosis with the 585-nm pulsed dye laser and local anesthesia. *Ann Otol Rhinol Laryngol* 2004;113:265–276.
33. Kimel S., Svaasand L.O., Milner T.E., et al. Laser photothermolysis of single blood vessels in the chick chorioallantoic membrane (CAM). *SPIE*; 1994. p. 216–27.
34. Anderson RR, Parrish JA. Selective photothermolysis: precise microsurgery by selective absorption of pulsed radiation. *Science* 1983;220:524–527.